

TMU-NT930301
March 1993

Pion Structure Function in the Nambu and Jona-Lasinio model

Takayuki Shigetani*, Katsuhiko Suzuki and Hiroshi Toki†

Department of Physics, Tokyo Metropolitan University

Hachiohji, Tokyo 192, Japan

(Phys. Lett. **B308** (1993) 383)

Abstract : The pion structure function is studied in the Nambu and Jona-Lasinio (NJL) model. We calculate the forward scattering amplitude of a virtual photon from a pion target in the Bjorken limit, and obtain valence quark distributions of the pion at the low energy hadronic scale, where the NJL model is supposed to work. The calculated distribution functions are evolved to the experimental momentum scale using the Altarelli-Parisi equation. The resulting distributions are in a reasonable agreement with experiment. We calculate also the kaon structure function and compare the ratio of kaon to pion valence u-quark distributions with experiment.

*e-mail address : shige@atlas.phys.metro-u.ac.jp

†Also at RIKEN, Wako, Saitama, 351, Japan

Recent experimental observations of deep inelastic scattering (DIS) provide us with a large amount of data about the structure of hadrons. These results [1, 2] indicate that our understanding of hadron structure is still incomplete. Quantum chromodynamics (QCD) is believed to be the theory of the strong interaction, and perturbative QCD is consistent to the measured Q^2 dependence of the structure function [3]. However, QCD is not able to predict directly the structure function itself, since non-perturbative effects of confinement and dynamical symmetry breaking are not yet understood in the context of QCD. On the other hand, phenomenological quark models, which possess some non-perturbative features of QCD, give remarkable predictions of static hadron properties such as masses and magnetic moments. Hence, it is of our great interest to clarify a connection between the DIS phenomena and the low energy non-perturbative features in terms of such models as effective theories of QCD. Such a connection would enable us to use the DIS data to constrain the models of low energy QCD.

Recently, the nucleon structure functions are discussed in terms of the MIT bag mode [4, 5] as well as other models [6]. Those results are based on the assumption that the structure functions at low energy hadronic scale $Q^2 = Q_0^2$ (unknown) are obtained by calculating the twist 2 matrix elements within the effective models, since the twist 2 operators are dominant in the Bjorken limit and higher twist terms vanish at high enough Q^2 [4]. Once one obtains them at the hadronic scale, these parton distributions are evolved to the experimental scale by using the perturbative QCD, and the comparison with experiment can be made.

In this letter, we concentrate on the pion structure function. The pion is believed to be the Goldstone boson due to the spontaneous breakdown of the chiral symmetry (SB χ S). Thus, the information of the pion structure function gives us deeper understandings of SB χ S. The experimental data of the pion structure function are extracted from πN scattering using the Drell-Yan process [7]. The valence, sea quark, and gluon distribution functions are obtained from a recent re-analysis of these data [8].

We use the Nambu and Jona-Lasinio (NJL) model [9], where the chiral invariance is

the main ingredient. The NJL model describes the pion as a collective $q\bar{q}$ excitation of the non-perturbative QCD vacuum [10]. Recently, the generalized $SU(3)_f$ NJL model with the $U(1)_A$ anomalous term is demonstrated to reproduce the meson properties successfully, in spite of the lack of confinement [10, 11, 12]. This model is also applied to the chiral phase transition at finite temperature and density [13]. All these results indicate that the NJL model possesses the essential features of QCD dynamics.

The $SU(3)_f$ NJL lagrangian is given by [10, 11, 12]

$$\begin{aligned}\mathcal{L}_{NJL} = & \bar{\psi}(i\gamma^\mu\partial_\mu - m)\psi \\ & + G_S[(\bar{\psi}\lambda_i\psi)^2 + (\bar{\psi}i\gamma_5\lambda_i\psi)^2] - G_V[(\bar{\psi}\gamma_\mu\lambda_i\psi)^2 + (\bar{\psi}\gamma_\mu\gamma_5\lambda_i\psi)^2],\end{aligned}\quad (1)$$

where ψ denotes the quark field with current mass m , λ_i are $SU(3)$ flavor matrices, and G_S , G_V are the coupling constants. In this model, the quarks acquire the constituent masses dynamically due to SB χ S. The meson masses are obtained by solving the Bethe-Salpeter equation. This model describes the $SU(3)_f$ meson properties very well with the parameters fixed by the pion and kaon properties [10, 11, 12]. Using this lagrangian, we will calculate the parton distribution of pion with no free parameter.

Unfortunately, the NJL model is a non-renormalizable theory, and this model requires the finite momentum cutoff $\Lambda \sim 1$ GeV, which is identified with a scale of SB χ S. One may understand the physical meaning of the cutoff as an approximate realization of "asymptotic freedom" in the NJL model. This means that the interaction between two quarks with the relative momentum larger than Λ is turned off, and two particles are free in such a high momentum scale. Hence, the structure functions obtained in the NJL model exhibit the Bjorken scaling in the deep inelastic limit [11]. If we use the cutoff in a Lorentz invariant manner, we can calculate the quark distributions as a function of the Bjorken x .

As mentioned above, we would like to calculate the structure function in the NJL model at a boundary to the QCD perturbation. The hadronic tensor $W_{\mu\nu}$ is written by

the structure functions F_1 and F_2 in the scaling limit;

$$\begin{aligned} W_{\mu\nu} = & - (g_{\mu\nu} - \frac{q_\mu q_\nu}{q^2}) F_1(x) \\ & + \frac{1}{m_\pi \nu} (p_\mu - \frac{p \cdot q}{q^2} q_\mu) (p_\nu - \frac{p \cdot q}{q^2} q_\nu) F_2(x) , \end{aligned} \quad (2)$$

where

$$F_2(x) = x \sum_i e_i^2 [q_i(x) + \bar{q}_i(x)] , \quad F_1(x) = \frac{F_2(x)}{2x} .$$

$q_i(x)$ and $\bar{q}_i(x)$ are the momentum distributions of the i -flavor quark and antiquark. The hadronic tensor is related to the forward scattering amplitude $T_{\mu\nu}$ through the optical theorem [3].

$$W_{\mu\nu} = \frac{1}{2\pi} \text{Im} T_{\mu\nu} . \quad (3)$$

Thus, we evaluate $T_{\mu\nu}$ in the NJL model to get the structure functions. The forward scattering amplitude of a virtual photon with q from a pion is defined by

$$T_{\mu\nu} = i \int d^4\xi e^{iq\xi} \langle p | T[J_\mu(\xi) J_\nu(0)] | p \rangle_C , \quad (4)$$

where $|p\rangle$ is a pion state of momentum p_μ , and q_μ the momentum delivered by the current. The current is $J_\mu = \bar{\psi} \gamma_\mu Q \psi$ with Q being the charge operator. We compute the "handbag diagrams" for $T_{\mu\nu}$, which is illustrated in fig.1a and 1b. The matrix element (4) in the NJL model is given by

$$T_{\mu\nu} = i \int \frac{d^4k}{(2\pi)^4} \text{Tr} [\gamma_\mu Q \frac{1}{k} \gamma_\nu Q T_-] + T_+ \text{ term} , \quad (5)$$

where

$$T_- = S_F(k - q)g_{\pi qq}\tau_+i\gamma_5S_F(k - q - p)g_{\pi qq}\tau_-i\gamma_5S_F(k - q) . \quad (6)$$

Here, $g_{\pi qq}$ is the coupling constant among two quarks and a pion obtained in the NJL model [10, 11, 12], and $\tau_{\pm} = (\tau_1 \pm i\tau_2)/\sqrt{2}$. T_- and T_+ denote scattering of a pion from quark and antiquark, respectively, where T_+ has a similar expression as (6). Note that the quark propagator contained in T_- has the dynamically generated mass obtained by solving the gap equation [9, 10]. Thus, $S_F(k)$ is written as

$$S_F(k) = \frac{1}{k - M} ,$$

where M is the constituent quark mass.

The structure function obtained by the calculation of the "handbag diagram", shown in figs.1a and 1b, coincides with the leading twist contribution of the operator product expansion in the Bjorken limit [14]. Therefore, these diagrams are enough for our purpose, because the structure functions are dominated by the twist 2 contributions in the DIS limit. Higher twist terms may be negligible at sufficiently high Q^2 [4].

Following the work of Landshoff *et al.* [15], we will carry out the integration of (5) in the Bjorken limit;

$$Q^2 = -q^2 \rightarrow \infty , \quad \nu = \frac{p \cdot q}{m_\pi} \rightarrow \infty , \quad x = \frac{Q^2}{2m_\pi\nu} : \text{fixed} .$$

Here x is the so-called Bjorken x , and m_π the pion mass. We introduce the integral variables

$$k_\mu = zp_\mu + yq_\mu + \kappa_\mu , \quad (7)$$

where κ_μ satisfies $\kappa \cdot p = \kappa \cdot q = 0$. Thus, κ_μ is spacelike ($\kappa^2 < 0$) and is effectively two dimensional. Calculating the traces and neglecting irrelevant terms in the Bjorken limit [15], we obtain

$$T_{\mu\nu} = \frac{8}{9} \frac{i}{(2\pi)^4} N_c g_{\pi qq}^2 \int dz d\bar{y} d^2\kappa \left(-g_{\mu\nu} + \frac{2z}{m_\pi \nu} p_\mu p_\nu + \frac{1}{m_\pi \nu} (p_\mu q_\nu + p_\nu q_\mu) \right) \times [t_1(\mu^2, s) + z t_2(\mu^2, s)] \frac{1}{z - x} , \quad (8)$$

where

$$t_1(\mu^2, s) = \frac{1}{(\mu^2 - M^2 + i\varepsilon)^2} \frac{1}{s - M^2 + i\varepsilon} (\mu^2 - M^2) ,$$

$$t_2(\mu^2, s) = \frac{1}{(\mu^2 - M^2 + i\varepsilon)^2} \frac{1}{s - M^2 + i\varepsilon} (s - M^2 - p^2)$$

and

$$\mu^2 = (k - q)^2 = z\bar{y} + \kappa^2 ,$$

$$s = (k - q - p)^2 = (z - 1)(\bar{y} - m_\pi^2) + \kappa^2 .$$

We change the variable $\bar{y} = 2m_\pi\nu(y - 1) + zp^2$ [15], and μ^2 and s are the invariant masses of the struck quark and spectator. Performing the z-integral in eq.(8), we find [15, 11]

$$T_{\mu\nu} = -\frac{8}{9} \frac{1}{(2\pi)^3} N_c g_{\pi qq}^2 \left[-g_{\mu\nu} + \frac{2z}{m_\pi \nu} p_\mu p_\nu + \frac{1}{m_\pi \nu} (p_\mu q_\nu + p_\nu q_\mu) \right] \times \int d\bar{y} d^2\kappa [t_1(\mu^2, s) + z t_2(\mu^2, s)] . \quad (9)$$

Consider now the \bar{y} -integral in the complex \bar{y} -plane. The s -propagator has a pole at $\bar{y} = (\kappa^2 - M^2)/(1 - x) + m_\pi^2 + i\varepsilon/(1 - x)$, and the μ -propagator has a double pole at

$\bar{y} = (M^2 - \kappa^2)/x - i\varepsilon/x$. For $x > 1$ or $x < 0$, all these singularities occur on the same side of the real \bar{y} -axis, and (9) gives a zero result [15, 14]. However, if $0 \leq x \leq 1$, the integration over \bar{y} no longer vanishes. Integrating (9) by \bar{y} and taking the imaginary part, we can get the quark distribution by use of the optical theorem (3). We change the integral variable k to μ^2 , we find the following expression for the quark distribution:

$$q(x) \propto -g_{\pi qq}^2 \int d\mu^2 \left[\frac{1}{\mu^2 - M^2} - x \frac{p^2}{(\mu^2 - M^2)^2} \right] \times \theta(m_\pi^2 x(1-x) - xM^2 - (1-x)\mu^2). \quad (10)$$

Here, θ is the usual step function which arises from the spacelike condition of κ . It is easily shown that the structure functions obtained from (10) exhibit the Bjorken scaling [11]. We identify (10) as the valence quark distribution of the pion $q_V(x)$, with the normalization $\int_0^1 dx q_V(x) = 1$. The integral (10) goes to infinity due to the non-renormalizability of the NJL model. Thus, we shall use the momentum cutoff. There exists an ambiguity in the introduction of the NJL cutoff for DIS phenomena [16, 17]. We introduce the Euclidean momentum, $t_E^2 = -\mu^2 + m_\pi^2 x - xM^2/(1-x)$, and simply assume that the four momentum of the struck quark has the sharp Euclidean cutoff, $\theta(\Lambda^2 - t_E^2)$, which is consistent to the NJL cutoff. We examine also the exponential cutoff used in ref.[16] and other plausible forms for completeness. We obtain similar results with ours except for the behavior of $q(x)$ around $x \sim 1$ which depends on the cutoff scheme.

Integrating (10) by $t_E(\mu^2)$ with the cutoff, we obtain the valence distribution of pion at the low energy hadronic scale, which is shown in fig.2. Here, we use the NJL parameters fixed by the pseudoscalar meson properties $\Lambda = 900\text{MeV}$, $G_S\Lambda^2 = 2G_V\Lambda^2 = 4.67$, $m_u = m_d = 5.5\text{MeV}$ and $m_s = 135\text{MeV}$ [10, 11, 12]. With this parameter set, we obtain the constituent masses, $M_u = M_d = 350\text{MeV}$ and $M_s = 534\text{MeV}$. Our results on the quark distribution depend only slightly on the choice of the parameters within the reasonable parameter ranges, once these parameters are constrained by the pion mass and the decay constant. Note that the resulting distribution shows a correct behavior around $x \sim 1$

; $q_V(x) \rightarrow 0$ as $x \rightarrow 1$ [11]. It is the advantage of our use of the NJL model, which is Lorentz invariant, as compared with the MIT bag model where the translational invariance is broken [5]. We also note that this low energy scale structure function has no physical meaning at this scale, since "real" structure function at the low energy scale receives non-negligible contributions from all twist operators. Our calculated result in fig.2 plays a role of only the boundary condition of the structure function for the Q^2 evolution.

We take the low energy hadronic scale at $Q_0^2 = (0.5\text{GeV})^2$, which is used in ref.[18]. At this scale, the running coupling constant is still small; $\alpha_s(Q_0^2)/\pi \sim 0.3$. Indeed, the inclusion of the second order QCD corrections gives a small change for the Q^2 evolution from our result within 10% [18]. We may understand intuitively the physical implication of this scale Q_0^2 as compared to the valence quark core radius of the pion $\langle r^2 \rangle_{core}$, noted by Brown et al. [19]. Their value is consistent to our low energy scale:

$$\langle r^2 \rangle_{core} \sim (0.35\text{fm})^2 \sim 1/(0.5\text{GeV})^2 .$$

We use the first order Altarelli-Parisi equation [20, 3] for the Q^2 evolution of valence distributions with $\Lambda_{QCD} = 250\text{MeV}$. We show in fig.2 (solid curve) the result at $Q^2 = 20\text{GeV}^2$, which is compared with the experimental curve (dash-dotted curve) extracted from the Drell-Yan process [8]. We find a reasonable agreement with experiment. If we vary the low energy scale Q_0^2 to a larger value $Q_0^2 = (0.75\text{GeV})^2$, the change of our distribution is of order 20 distribution function at the experimental scale, it seems necessary to choose Q_0^2 as small as $Q_0^2 = (0.5\text{GeV})^2$. We compare the pion structure function $F_\pi(x)$ with the experiment in fig.3. It shows a good agreements for $x > 0.3$. In the low x region, the structure function is dominated by the sea quark distribution [3]. We ought to calculate the sea quark contributions [16, 17] with the next-to-leading order QCD perturbation, which is under consideration.

We also calculate the first two moments of the valence quark distributions, $\langle x \rangle$ and

$\langle x^2 \rangle$, which are defined as

$$\langle x \rangle = \int_0^1 dx x q_v(x) , \quad \langle x^2 \rangle = \int_0^1 dx x^2 q_v(x) .$$

The resulting values are shown in table 1 with the experimental values [8] and the results of the lattice QCD calculations [21]. Our results reproduce the data very well.

Finally, we discuss the kaon structure function. We can extract the effects of the SU(3) flavor symmetry breaking from quark distributions of the kaon. The valence quark distributions are obtained in a similar manner using the NJL model. The u- and s-quark distributions of the kaon at the low momentum scale and those at $Q^2 = 20 \text{GeV}^2$ are shown in fig.4. Our results indicate that the heavy s-quark carries a larger fraction of kaon momentum than the light u(d) quark, as expected. The resulting distributions show a similar behavior with the previous results obtained by the analysis of the Regge trajectories [22]. We also show in fig.5 the ratio of kaon to pion valence u-quark distributions u_K/u_π at $Q^2 = 20 \text{GeV}^2$ with experimental data [23]. This ratio is sensitive to the mass difference of the constituent quark masses. In fact, our calculations give a simple expression of this ratio around $x \sim 1$ at the low momentum scale as

$$u_K/u_\pi \sim (M_u/M_s)^2 \sim 0.5 .$$

This value is quite reasonable in view of the experimental findings.

In conclusion, we have studied the pion structure function at the DIS scale using the NJL model as a low energy effective theory of QCD. The resulting distribution at the low momentum scale is evolved to the experimental scale, at which it compares with the DIS data very well. We have also studied the kaon structure function. Reflecting the SU(3) flavor symmetry breaking due to the bare current mass difference, the x dependence of the ratio of kaon to pion valence u-quark distributions is found consistent with experiment. Our results indicate that the low energy effective quark model is able to describe the DIS

phenomena. We shall point out that the sea quark degrees of freedom can be naturally included in the framework of the NJL model, which is needed to compare with the pion structure function directly. It is possible to calculate the sea quark distributions in the NJL model as higher loop corrections [16, 17].

We are grateful to T. Hatsuda and T. Kobayashi for illuminating discussions on the deep inelastic phenomena.

References

- [1] M. Arneodo, preprint: CERN PPE/92-113
EM Coll., J. Ashman et al., Nucl. Phys. **B328** (1989) 1
- [2] NM Coll., P. Amaudruz et al., Phys. Rev. Lett. **66** (1991) 2716;
For a review, B. Badelek et al., Rev. Mod. Phys. **64** (1992) 927
- [3] E. Reya, Phys. Rev. **69** (1981) 195
R.L. Jaffe, Lectures presented at the 1985 Los Alamos School on Quark Nuclear Physics, June 10-14, 1985
- [4] R.L. Jaffe and G.G. Ross, Phys. Lett. **B93** (1980) 313
- [5] C.J. Benesh and G.A. Miller, Phys. Rev. **D36** (1987) 1344
A.W. Schreiber, A.I. Signal and A.W. Thomas, Phys. Rev. **D44** (1991) 2653, and references therein.
- [6] L.S. Celenza and C.M. Shakin, Phys. Rev. **C27** (1983) 1561
C.J. Benesh and G.A. Miller, Phys. Lett. **B215** (1988) 381
R.P. Bickerstaff and T. Londergan, Phys. Rev. **D42** (1990) 3621
H. Meyer and P.J. Mulders, Nucl. Phys. **A528** (1991) 589
- [7] NA3 Coll., J. Badier et al., Z. Phys. **C18** (1983) 281
NA10 Coll., B. Betev et al., Z. Phys. **C28** (1985) 15
E537 Coll., E. Anassontzis et al., Phys. Rev. **D38** (1988) 1377
E615 Coll., P. Bordalo et al., Phys. Lett. **B193** (1987) 368
WA70 Coll., M. Bonesini et al., Z. Phys. **C37** (1988) 535
- [8] P.J. Sutton, A.D. Martin, R.G. Roberts and W.J. Stirling, Phys. Rev. **D45** (1992) 2349
- [9] Y. Nambu and G. Jona-Lasinio, Phys. Rev. **122** (1961) 345, *ibid.* **124** (1961) 246

[10] For recent reviews; U. Vogl and W. Weise, *Prog. Part. Nucl. Phys.* **27** (1991) 195, S.P. Klevansky, *Rev. Mod. Phys.* **64** (1992) 649, and references therein.

[11] V. Bernard, R.L. Jaffe and U.-G. Meissner, *Nucl. Phys.* **B308** (1988) 753

[12] T. Hatsuda and T. Kunihiro, *Z. Phys.* **C51** (1991) 49
 M. Takizawa, K. Tsushima, Y. Kohoyama and K. Kubodera, *Nucl. Phys.* **A507** (1990) 611
 S. Klimt, M. Lutz, U. Vogl and W. Weise, *Nucl. Phys.* **A516** (1990) 429

[13] T. Hatsuda and T. Kunihiro, *Phys. Lett.* **B145** (1984) 7; *Phys. Lett.* **B185** (1987) 304
 V. Bernard, U.-G. Meissner and I. Zahed, *Phys. Rev.* **D36** (1987) 819

[14] A. De Rújula and F. Martin, *Phys. Rev.* **D22** (1980) 1787

[15] P. V. Landshoff, J. C. Polkinghorne and R. D. Short, *Nucl. Phys.* **B28** (1971) 225

[16] C.L. Korpa and U.-G. Meissner, *Phys. Rev.* **D41** (1990) 1679

[17] M. Burkardt and B.J. Warr, *Phys. Rev.* **D45** (1992) 958

[18] M. Glück, E. Reya and A. Vogt, *Z. Phys.* **C53** (1992) 651

[19] G.E. Brown, M. Rho and W. Weise, *Nucl. Phys.* **A454** (1986) 669

[20] G. Altarelli and G. Parisi, *Nucl. Phys.* **B126** (1977) 298

[21] G. Martinelli and C.T. Sachrajda, *Nucl. Phys.* **B306** (1988) 865

[22] P.V. Chliapnikov et al., *Nucl. Phys.* **B148** (1979) 400
 A. El Hassouni and O. Napoly, *PR D23* 1981 193

[23] J. Badier et al., *PL B93* 1980 354

Table Caption

Table 1 : The first two moments of the pion distribution at $Q^2 = 49 GeV^2$. The theoretical calculations of the NJL model are shown in the second row, and compared with the experimental values [8] (third row) and the lattice QCD results [21] (last row).

Table 1

	$2\langle x \rangle$	$2\langle x^2 \rangle$
Theory	0.41	0.16
Experiment	0.40 ± 0.02	0.16 ± 0.01
Lattice	0.46 ± 0.07	0.18 ± 0.05

Figure Captions

Fig. 1 : The forward Compton scattering amplitude ("handbag diagram") of the pion.

The solid line represents the quark. The pion and the virtual photon are depicted by the dashed and wavy lines. For details and notation, see text.

Fig. 2 : The valence quark distributions of the pion at the low energy scale $Q^2 = Q_0^2$ (dotted curve) and at $Q^2 = 20GeV^2$ (solid curve) as a function of the Bjorken x .

The experimental fit [8] is depicted by the dash-dotted curve.

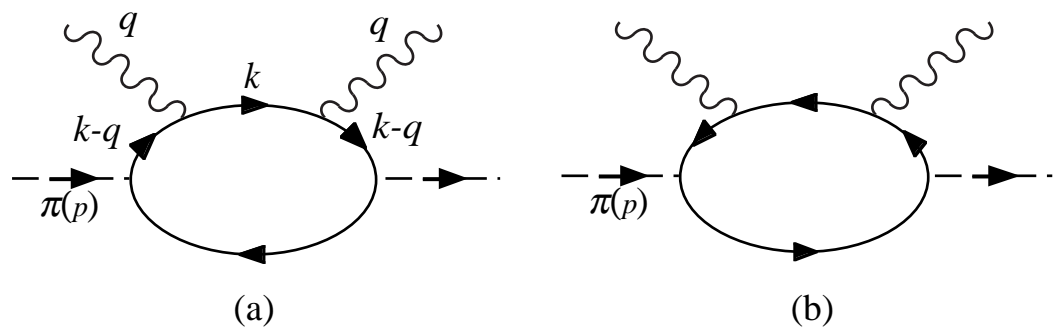
Fig. 3 : The pion structure function at $Q^2 = 20GeV^2$. The experimental data are taken from the NA3 experiment [7]. The theoretical prediction of the NJL model is depicted by the solid curve. Here, we use $F_\pi(x) = Kxq_V(x)$ with the sea quark distributions being neglected, where we take the K -factor, $K=1.5$ [8].

Fig. 4 : The valence quark distributions of the kaon at low energy scale and at $Q^2 = 20GeV^2$ in the NJL model. The u- and s-quark distribution at Q_0^2 are depicted by the dotted and dashed curves. The solid and dashed-dotted curves represent the u- and s-quark valence distributions at $Q^2 = 20GeV^2$.

Fig.5 : The ratio of kaon to pion valence u-quark distributions

u_K/u_π at $Q^2 = 20GeV^2$ scale. The theoretical result is depicted by the solid curve. The experimental values with error bars are taken from ref.[23].

Fig. 1



This figure "fig1-1.png" is available in "png" format from:

<http://arxiv.org/ps/hep-ph/9402286v1>

This figure "fig2-1.png" is available in "png" format from:

<http://arxiv.org/ps/hep-ph/9402286v1>

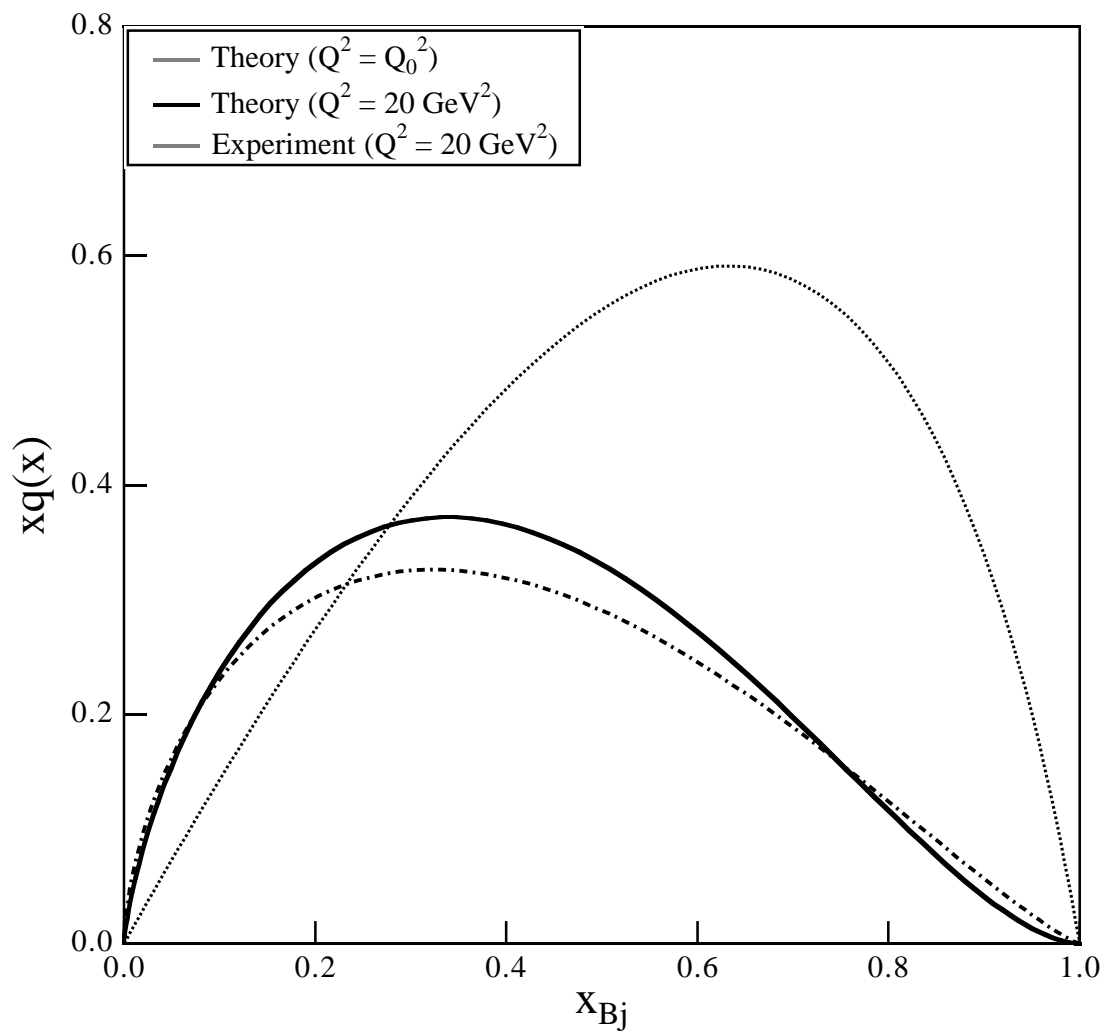


Fig.2

This figure "fig1-2.png" is available in "png" format from:

<http://arxiv.org/ps/hep-ph/9402286v1>

This figure "fig2-2.png" is available in "png" format from:

<http://arxiv.org/ps/hep-ph/9402286v1>

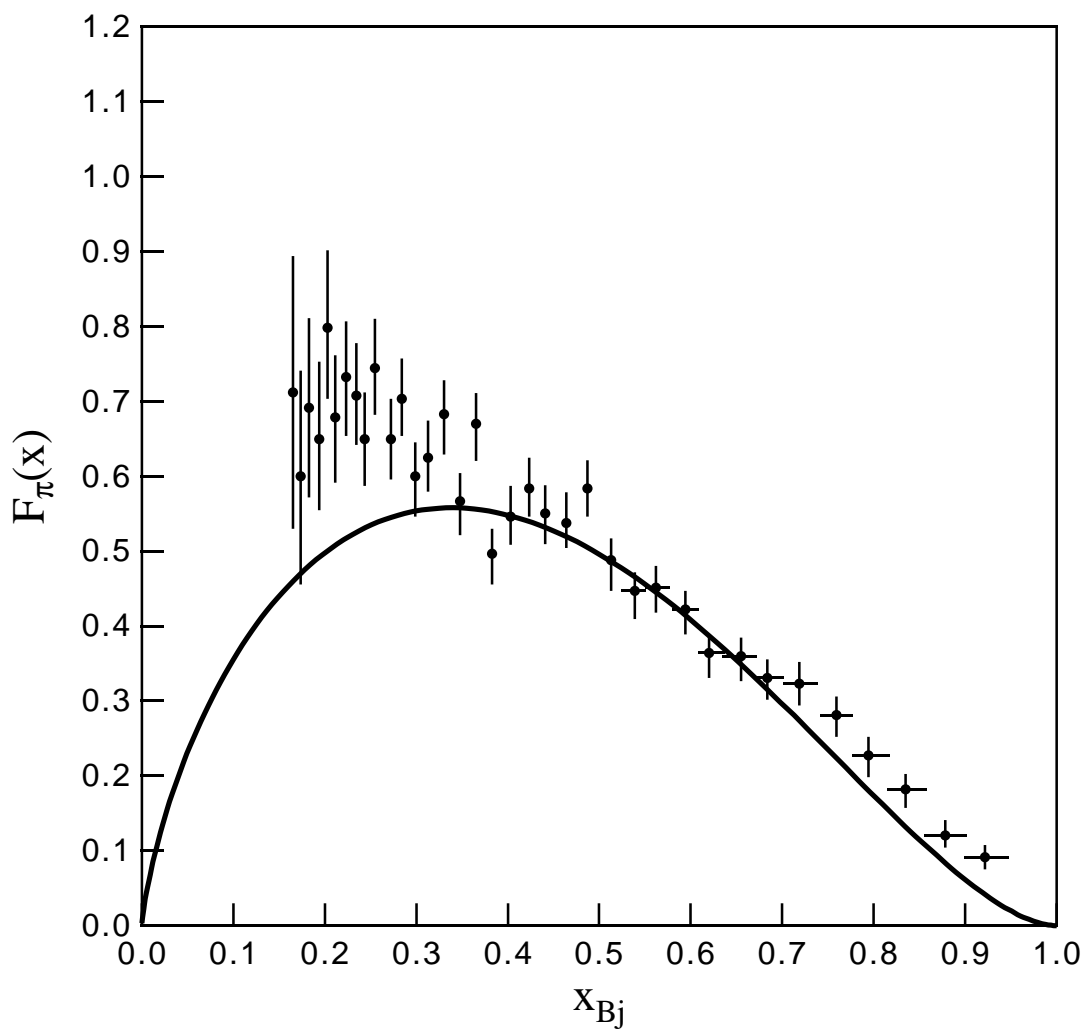


Fig.3

This figure "fig1-3.png" is available in "png" format from:

<http://arxiv.org/ps/hep-ph/9402286v1>

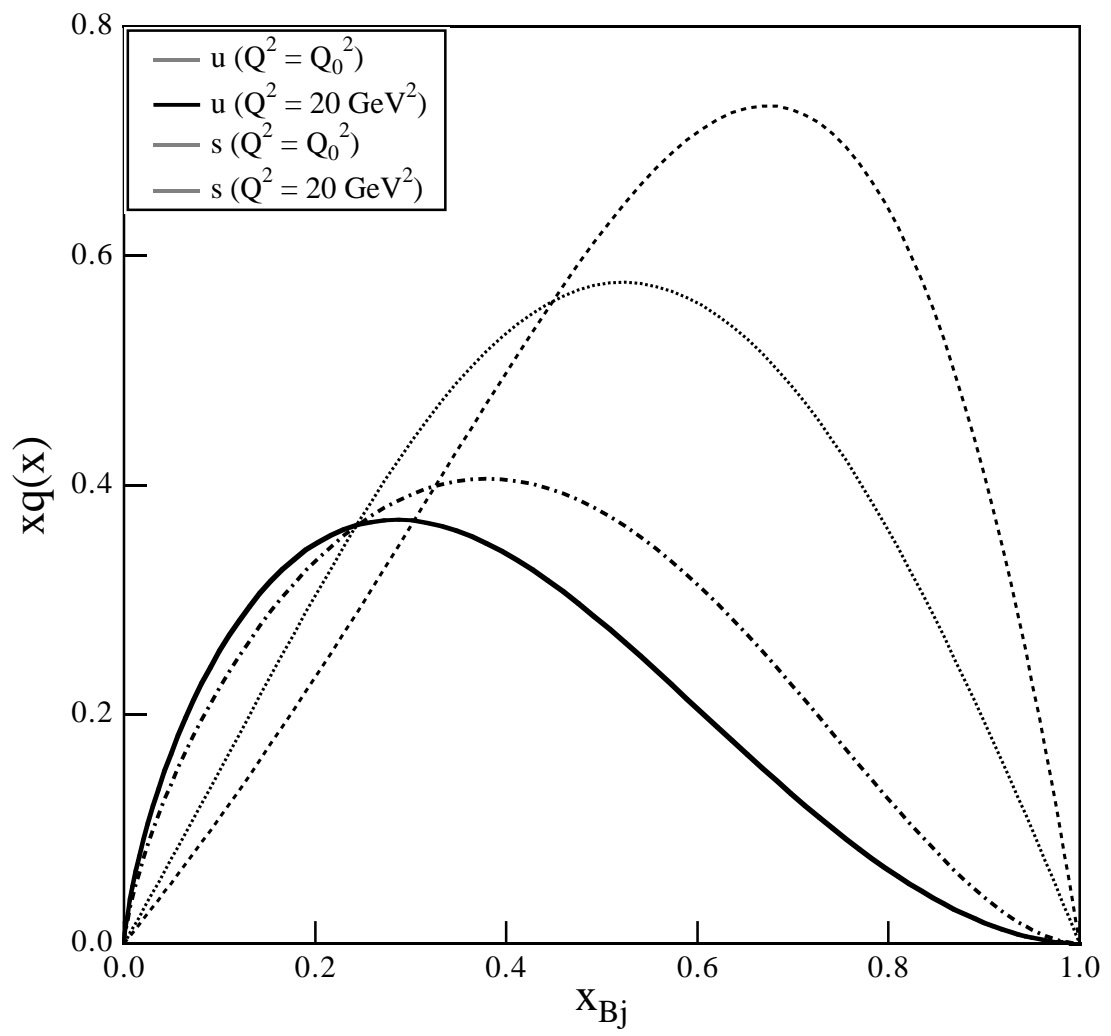


Fig.4

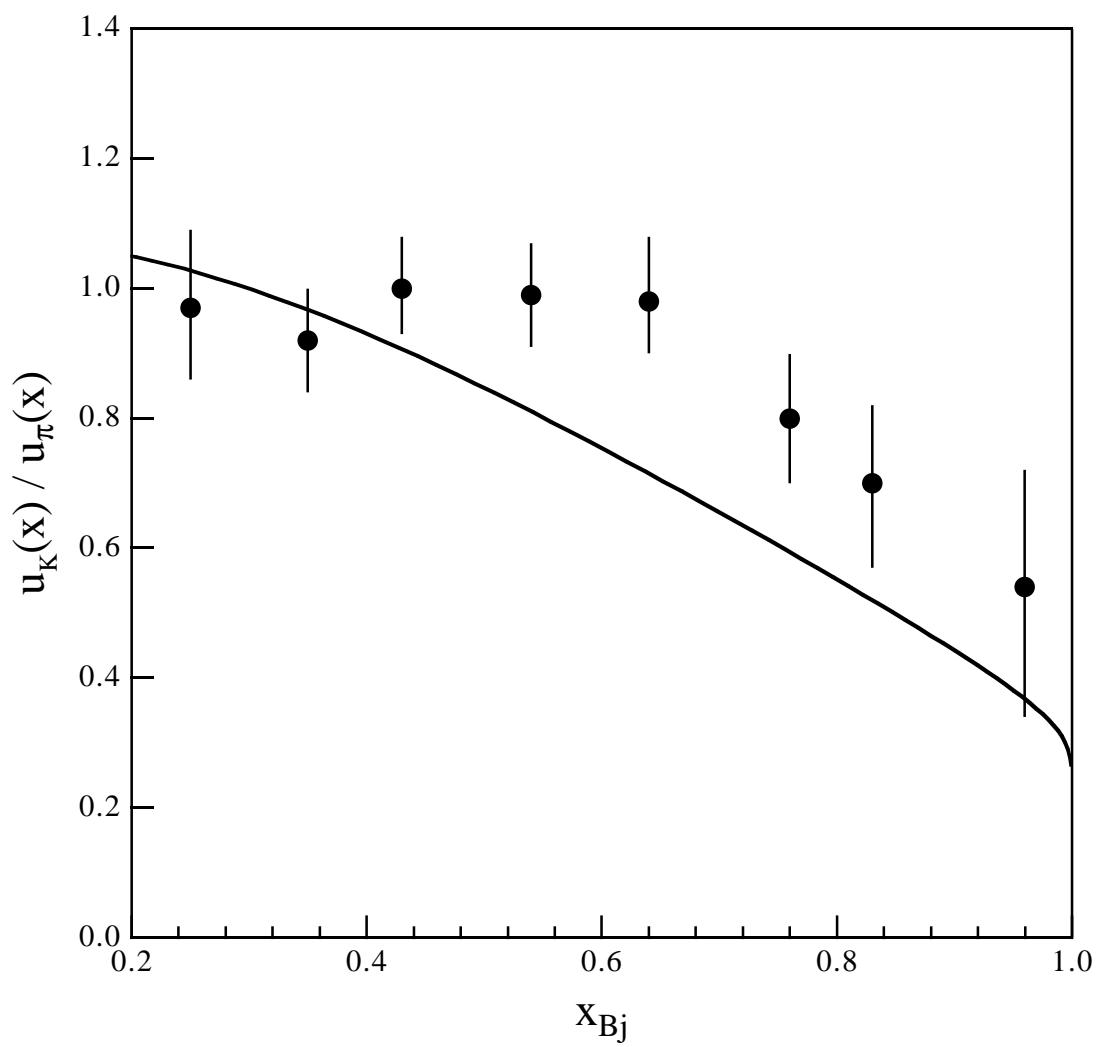


Fig.5